Variation of Shear Wave Elastography With Preload in the Thyroid

Ozturk Arinc (Orcid ID: 0000-0002-5335-3737)
Grajo Joseph (Orcid ID: 0000-0002-9704-2447)
Samir Anthony (Orcid ID: 0000-0002-7604-9260)
Zubajlo Rebecca (Orcid ID: 0000-0001-9051-5275)

Variation of Shear Wave Elastography with Preload in the Thyroid: Quantitative Validation

Arinc Ozturk, MD*[1]; Rebecca E. Zubajlo, MS*[2]; Manish Dhyani, MD[3]; Joseph R. Grajo, MD[4]; Nathaniel Mercaldo, PhD[5]; Brian W. Anthony, PhD[2], Anthony E. Samir, MD, MPH[1]
*Co-first authors

1- Center for Ultrasound Research & Translation, Department of Radiology, Massachusetts General Hospital, Boston, MA, USA, 02114
2- Department of Mechanical Engineering, Massachusetts Institutes of Technology, Cambridge, Massachusetts, USA, 02139
3- Department of Radiology, Lahey Hospital & Medical Center, Burlington, Massachusetts, USA, 01805
4- Division of Abdominal Imaging, Department of Radiology, University of Florida College of Medicine, Gainesville, Florida, USA, 32610
5- Department of Neurology, Massachusetts General Hospital, Boston, MA, USA, 02114

Manuscript Category: Original Research
Short Running Title: Quantification of Thyroid Elastography Variation

Corresponding Author Until Publication: Rebecca E. Zubajlo, M.S.
Mailing address: 32 Vassar Street, 35-231, Cambridge, MA 02139
Telephone: 301-676-0926
Email: rzubajlo@mit.edu

Corresponding Author After Publication: Anthony E. Samir, MD, MPH
Mailing address: Center for Ultrasound Research & Translation, 101 Merrimac St. 3rd floor. Rm 328, Boston, MA, 02114.
Telephone: 617-643-2009
Email: asamir@mgh.harvard.edu

This is the author manuscript accepted for publication and has undergone full peer review but has not been through the copyediting, typesetting, pagination and proofreading process, which may lead to differences between this version and the Version of Record. Please cite this article as doi: 10.1002/jum.15456

ABSTRACT

Objectives: Thyroid shear wave elastography (SWE) has been shown to have advantages compared to biopsy or other imaging modalities in the evaluation of thyroid nodules. However, studies show variability in its assessment. The objective of this study was to evaluate if stiffness measurements of the normal thyroid, as estimated by SWE, varied due to preload force, or the pressure applied between the probe and the patient. **Methods:** In this study, a measurement system was attached to the ultrasound probe to measure applied load. Shear wave elastography measurements were obtained from the left lobe of the thyroid at applied probe forces between 2 and 10 Newtons (N). A linear mixed effects model was constructed to quantify the association between preload force and stiffness while accounting for correlations between repeated measurements within each subject. Preload force effect on elasticity was modeled using both a linear and quadratic term to account for possible non-linear association between these variables. **Results:** Nineteen healthy subjects without known thyroid disease participated in the study. Subjects were 36 ± 8 years of age, 74% female, 74% normal BMI, and 95% white non-Hispanic/Latino. Estimated elastography values at 2 N preload force were 16.7 kPA [95% CI: 14.1, 19.3] whereas the values at 10 N were 29.9 kPa [24.9, 34.9]. **Conclusions:** Preload force was significantly, and non-linearly, associated with SWE estimates of thyroid stiffness. Quantitative standardization of preload forces in the assessment of thyroid nodules using elastography is an integral factor for improving accuracy of thyroid nodule evaluation.

Keywords: *shear wave elastography, quantitative ultrasound, preload force, thyroid nodule, transducer augmentation*

INTRODUCTION

Ultrasound imaging modalities are commonly used for thyroid nodule evaluation. Modern ultrasound imaging demonstrates thyroid nodules in up to 60% of adults.[1] Conventional B-mode ultrasound has good sensitivity for identifying potentially malignant nodules and is widely used for this purpose. Unfortunately, interpreting conventional ultrasound has limitations in differentiating benign and malignant lesions.[2] Several scientific consortia have developed decision-making guidelines regarding invasive testing after discover of a thyroid nodule.[3] Based on these guidelines, fine needle aspiration (FNA) is performed to determine whether a nodule is benign or malignant.[4] In 62 - 85% of aspirations, the nodule is cytologically diagnosed as benign and typically requires only periodic follow-up.[4] In 4 - 8%, the nodule is diagnosed as malignant and may require total thyroidectomy.[5] Unfortunately, in up to 25% of nodules the cytologic diagnosis is indeterminate, conferring a risk of malignancy of between 10 and 66%.[6] In these nodules, molecular aspirate testing has been shown to have a high negative predictive value but is costly and has low positive predictive value.[7,8] A less invasive alternative to these tests is ultrasound elastography.

Ultrasound elastography can measure and map thyroid nodule stiffness.[9] Two types of elastography have been used for this purpose: strain elastography (SE) and shear wave elastography (SWE), which can be further categorized into (i) point shear wave elastography (pSWE) and (ii) two-dimensional shear wave elastography (2D-SWE).[10] SE uses mechanical compression methods, based on manual pressure or pressure from adjacent arterial pulsation.[10]

Thyroid nodule SE can be interpreted using scoring systems published by Asteria[11] and Rago.[12] These systems rely on qualitative interpretation of elastogram morphologic features. For SE, the combination of inherently variable exogenous pressure and interpretative subjectivity result in poor interobserver agreement[13] and reports of low malignancy sensitivity and specificity.[14] Shear wave elastography (SWE) use acoustic radiation force generated by the ultrasound device to induce shear waves in a localized tissue. The propagation velocity of these shear waves can be measured and used to derive quantitative stiffness estimates.[15]

pSWE uses a single focal excitation point while 2D-SWE uses multiple focal points. pSWE has been shown to be useful for differentiating benign and malignant nodules, with a sensitivity of 80% and specificity of 85%.[16] Similar results have been shown for 2D-SWE thyroid nodule malignancy detection (82% sensitivity and 88% specificity).[17]

The reported performance of shear wave elastography for thyroid nodule malignancy detection is variable: for example, some studies have shown that SWE can differentiate benign and malignant nodules that are cytologically indeterminate[17] while other studies have not.[18] This variability may be related to measurement error produced by operator-applied transducer pressure, also termed preload. It is known ultrasound transducer pressure on the thyroid increases elastographic stiffness estimates.[19] This effect is widely known and is mitigated in liver imaging by insonation through the intercostal spaces.[20] Unlike the liver, the thyroid has no overlying ribs to protect it from compression by the overlying transducer and is superficial, and therefore prone to elastographic measurement error induced by transducer pressure. The objective of this study

was to evaluate if stiffness measurements of the normal thyroid, as estimated by thyroid shear wave elastography, varied due to preload force.

MATERIALS AND METHODS

Study Subjects

This institutional review board-approved, single-center, prospective study was compliant with the Health Insurance Portability and Accountability Act (HIPAA). Nineteen randomized, healthy volunteers without known thyroid disease participated in the study from May - August 2017. The sample size was chosen to exceed the minimum target of fourteen subjects. With a sample size of 14 subjects and a type-I error of 5%, we have 80% power to detect a correlation value of at least 0.70 between stiffness values and preload force (via Fisher's z-transformation). Volunteers younger than 18 years were excluded. Informed consent was obtained from participants who fulfilled the inclusion criteria before the ultrasound exam. All demographic data for the patient cohort is summarized in Table 1.

Force measurement

A series of custom, hand-held force measuring devices to augment commercially available ultrasound systems were developed by Massachusetts Institute of Technology (MIT).[21–23] Our device attaches to the Supersonic Imagine SL15-4 linear transducer by a quick-release, 3D-printed clamp (Figure 1). The device measures and records the contact force (force applied to the subject's

neck by the transducer) via a Futek Single Axis Load Cell (Futek FSH00095, Irvine CA) and orientation angles of the ultrasound transducer via an ADXL-335 tri-axial accelerometer (Analog Devices, Norwood MA) which measures the orientation of the probe with respect to gravity and enables compensation for probe mass. The total mass is approximately 200 g, similar to the mass of the ultrasound transducer and only increases the width of the device by 2 cm. A sampling rate of 100 Hz was used for the digital acquisition of force and transducer orientation within the custom LabVIEW (National Instruments, Austin TX) program, which runs on a tablet running Windows 10 (Microsoft, Seattle WA) where the measurements are displayed in real time. In the literature, the terms "contact force" (units: Newtons) and "contact pressure" (units: Newtons/meter^2) are often used interchangeably. The force measurement transducer directly measures force; therefore, force data are presented. Contact pressure is approximated by dividing the force by the contact area of the force measurement transducer, which is approximately 7.2 cm^2 (assuming full transducer face contact). Forces along the axis of the transducer (perpendicular to the transducer face) were more than an order of magnitude greater than forces applied in the other two directions. Therefore, only a single axis load cell was used to measure the force along the axis of the transducer (in the axial direction); all forces reported here were along this axial direction and specified in Newtons (N) (4.45 N = 1 lbf).

Ultrasound and elastography scan

All volunteers underwent a thyroid examination in a supine position by a single radiologist (YH) with over 10 years of thyroid ultrasound experience to exclude thyroid disease. Subsequently, all elastography examinations were performed using the same Aixplorer (Supersonic Imagine, Paris, France) ultrasound machine. Shear wave elastography acquisitions were repeated 5 times at increasing preload forces (2 N, 4 N, 6 N, 8 N, 10 N) using the SL15-4 transducer (Figure 2). This force interval (2 - 10 N) was chosen because was found to be the relevant force range applied in clinical settings, which ends around 10 N as it is the common maximum tolerable pressure of subjects with no discomfort. All measurements were made in the left thyroid lobe. All regions of interested were placed within the SWE image with a qualitative image scale extending from 0 to 100 kPa. The largest region of interest that could fit within the normal thyroid tissue was used to reduce potential sources of bias in the measurement. The average measured stiffness in the region of interest is the reported Young's modulus in kilopascals (kPa).

Statistical analysis

Demographic and stiffness (Young's modulus) summaries were calculated for the patient cohort. Categorical variables were summarized using frequencies and percentages, while continuous variables were summarized using quartiles (25, 50, 75th), means, and standard deviations (SD). A linear mixed-effects model was constructed to quantify the association between preload forces and Young's modulus values. This model included both random-intercepts and slopes to account for possible correlations arising from the multiple measurements per subject.

The random effects specification also acknowledged the nested nature of the multiple preload measurements within each subject. Possible confounding factors, such as age and gender, were not included as covariates due to the small sample size, but it was hypothesized that these covariates would not have an effect on Young's modulus values due to the homogeneity of the patient cohort. The preload force effect was modeled using both a linear and quadratic term to acknowledge nonlinear relationships. Fixed-effects estimates, and their 95% confidence intervals, were computed for all model parameters. Linear combinations of these parameters were used to estimate both mean Young's modulus values for preload forces (i.e., 2 N, 4 N) as well as sequential differences in these values (i.e., 4 N - 2 N). All statistical analyses were performed by a statistician (NM) using open source R software version 3.4.3.

RESULTS

Study Subjects

Table 1 summarizes the demographic statistics for the patient cohort. On average, these participants were 36.3 ($\pm$ 8.4) years old, primarily female (74%), of a normal body mass index (BMI) (74%) and non-Hispanic/Latino (95%).

Force measurement and elastography relation

The average stiffness (Young's modulus) values (kPa) increased as the preload force increased. For example, preload forces of 2 N and 4 N were, on average, associated with Young's

modulus values of 16.6 (± 5.1) kPa and 19.4 (± 7.2) kPa, respectively. As described in Table 2, for each subject and preload force value, five Young's modulus values were collected. Descriptive summaries of the average of these measurements were computed, including: the mean, standard deviation (SD), and the 25th, 50th (median), and 75th percentiles.

Regression coefficient estimates, estimated mean Young's modulus values, confidence intervals (CI), and differences in these values are presented in Table 3. The estimated coefficients associated with preload force (linear, quadratic) were positive and statistically different than zero indicating that the preload force and Young's modulus relationship was positive and non-linear. Estimated average Young's modulus values were 16.7 kPa [95% CI: 14.1, 19.3] and 29.9 kPa [24.9, 34.9] for preload forces 2 N and 10 N, respectively. Figure 3 depicts the non-linear relationship for all preload forces between 2 - 10 N. Sequential differences in Young's modulus values ranged from 2.6 kPa [1.3, 3.8] to 4.0 kPa [2.8, 5.3] when comparing 4 N - 2 N and 10 N - 8 N.

DISCUSSION

Conventional B-mode ultrasound (CUS) is low-cost, widely available and widely used for thyroid imaging. CUS can detect the presence of a nodule in up to 67% of the adult population.[24] However, CUS has variable sensitivity and specificity for thyroid nodule malignancy, ranging from 50% to 95%.[25] Many nodule sonographic features are subjective, leading to low agreement between ultrasound operators.[26] SWE estimates of nodule stiffness are higher in malignant than

benign nodules,[2,11,17,27] with reported SWE sensitivity and specificity for thyroid nodule malignancy of 80% - 86.3% and 85% - 89.5%, respectively.[10] SWE has also shown to have utility in diagnosing diffuse thyroid disease like Hashimoto's and Graves' disease.[28–30] While SWE is thought to be more operator-independent than strain elastography, it is known that applied force may confound SWE measurement.[31] Variation in applied force is a likely contributor to SWE measurement variability across studies,[32] making it challenging to define a SWE-measured nodule stiffness threshold for malignancy or disease state, limiting widespread use of SWE for thyroid nodule risk stratification in clinical practice.

Applied preload force results in tissue compression, which changes the elastic properties of the tissue and may lead to false incorrect diagnosis. This phenomenon has been observed in many tissues, including the breast, cervix, kidney, and thyroid.[2,33–36] The effect of preload on thyroid nodule elastography stiffness values has been examined in several studies, both in clinical and *ex-vivo* study settings.[2,31]

Considering the effect of pressure on thyroid tissue stiffness, there is a clear need for better understanding of the effects of applied preload when making diagnostic measurements. To our knowledge, no prior studies have reported a technique to quantify hand pressure force levels in SWE exam of the thyroid tissue in clinically relevant force ranges. In this study, we developed a custom device attached to a standard thyroid imaging transducer, successfully quantified the applied force, and presented a direct high temporal resolution association between applied force

and SWE-estimated thyroid tissue stiffness. This device can be used to inform the operator in performing standardized ultrasound exams.

There were several limitations in this study: [1] we imaged the thyroid in volunteers without known thyroid disease. It is possible that thyroid nodules or existing diffuse thyroid disease will exhibit a different response to preload. However, if anything, we anticipate that applied force will most likely show greater effects in encapsulated nodules than in the normal thyroid. A future analysis in subjects with benign and malignant thyroid nodules as well as diffuse thyroid disease would be ideal. We also did not perform blood tests for thyroid function but rather used ultrasound biomarkers to indicate thyroid health. In a future study, we can confirm the tissue health with blood biomarkers as well. [2] We did not control the results for the dimensions and composition of the subjects' overlying soft tissue. We report BMI and consider the sample representative of a typical imaging population; nonetheless, a larger cohort with a stratified analysis of the effects of neck thickness and BMI would be desirable. [3] We performed imaging on a single vendor's ultrasound platform. However, the physical basis of SWE is similar across commercially available ultrasound platforms and it is expected that results will be similar on other platforms.

The results present high temporal resolution quantitative estimate of the effect of applied force on normal thyroid tissue. Importantly, substantial changes in the Young's modulus measured via shear wave elastography were observed during scanning at forces shown to be within the range of forces typically applied during conventional sonographic imaging.[37] This is clinically important,

as it implies that the confounding effects of applied preload may play a role in limiting the generalizability of SWE for thyroid nodule malignancy risk detection and diffuse thyroid disease detection in clinical practice. This finding emphasizes the importance of accounting for preload in ultrasound particularly for the thyroid and in thyroid diseases. The increase in stiffness value indicated by ultrasound elastography may shift the elasticity of a benign nodule to a stiffness of a malignant nodule – requiring the patient to go through more invasive testing. The technology, ultrasound augmented with force sensing, we have developed to quantify this effect may provide a tool to mitigate this confounding effect in future.

ACKNOWLEDGMENTS

The authors would like to acknowledge the National Science Foundation GFRP, Athena Huang, Matthew Gilbertson, and Yibin Huang for their contributions to this work.

REFERENCES

1. Guth S, Theune U, Aberle J, Galach A, Bamberger CM. Very high prevalence of thyroid nodules detected by high frequency (13 MHz) ultrasound examination. *Eur J Clin Invest*. 2009;39(8):699-706.
2. Lyshchik A, Higashi T, Asato R, et al. Thyroid gland tumor diagnosis at US elastography 1. *Radiology*. 2005;237(1):202-211.
3. Tessler FN, Middleton WD, Grant EG, et al. ACR Thyroid Imaging, Reporting and data system (TI-RADS): white paper of the ACR TI-RADS committee. *J Am Coll Radiol*. 2017;14(5):587-595.
4. Wang C-CC, Friedman L, Kennedy GC, et al. A large multicenter correlation study of thyroid nodule cytopathology and histopathology. *Thyroid*. 2011;21(3):243-251.
5. Yassa L, Cibas ES, Benson CB, et al. Long-term assessment of a multidisciplinary approach to thyroid nodule diagnostic evaluation. *Cancer*. 2007;111(6):508-516.
6. Popoveniuc G, Jonklaas J. Thyroid nodules. *Med Clin North Am*. 2012;96(2):329-349.
7. Alexander EK, Kennedy GC, Baloch ZW, et al. Preoperative diagnosis of benign thyroid nodules with indeterminate cytology. *N Engl J Med*. 2012;367(8):705-715.
8. Bomeli SR, LeBeau SO, Ferris RL. Evaluation of a thyroid nodule. *Otolaryngol Clin North Am*. 2010;43(2):229-238, vii.
9. Ozturk A, Grajo JR, Dhyani M, Anthony BW, Samir AE. Principles of ultrasound elastography. *Abdom Radiol*. 2018;43(4):773-785.

10. Sigrist RMS, Liau J, Kaffas A El, Chammas MC, Willmann JK. Ultrasound elastography: Review of techniques and clinical applications. *Theranostics*. 2017;7(5):1303-1329.

11. Asteria C, Giovanardi A, Pizzocaro A, et al. US-elastography in the differential diagnosis of benign and malignant thyroid nodules. *Thyroid*. 2008;18(5):523-531.

12. Rago T, Santini F, Scutari M, Pinchera A, Vitti P. Elastography: New developments in ultrasound for predicting malignancy in thyroid nodules. *J Clin Endocrinol Metab*. 2007;92(8):2917-2922.

13. Koh J, Moon HJ, Park JS, et al. Variability in interpretation of ultrasound elastography and gray-scale ultrasound in assessing thyroid nodules. *Ultrasound Med Biol*. 2016;42(1):51-59.

14. Moon HJ, Sung JM, Kim E-K, Yoon JH, Youk JH, Kwak JY. Diagnostic performance of gray-scale US and elastography in solid thyroid nodules. *Radiology*. 2012;262(3):1002-1013.

15. Garra BS. Elastography: history, principles, and technique comparison. *Abdom Imaging*. 2015;40(4):680-697.

16. Zhan J, Jin J-M, Diao X-H, Chen Y. Acoustic radiation force impulse imaging (ARFI) for differentiation of benign and malignant thyroid nodules—A meta-analysis. *Eur J Radiol*. 2015;84(11):2181-2186.

17. Samir AE, Dhyani M, Anvari A, et al. Shear-wave elastography for the preoperative risk stratification of follicular-patterned lesions of the thyroid: Diagnostic accuracy and

optimal measurement plane. *Radiology*. 2015;277(2):565-573.

18. Bardet S, Ciappuccini R, Monpeyssen H, Jj M, Tissier F, Blanchard D. Shear wave elastography in thyroid nodules with indeterminate cytology : results of a prospective bicentric study. *Thyroid*. 2017;27(11).
19. Dudea SM, Botar-Jid C. Ultrasound elastography in thyroid disease. *Med Ultrason*. 2015;17(1):74-96.
20. Ferraioli G, Filice C, Castera L, et al. WFUMB guidelines and recommendations for clinical use of ultrasound elastography: Part 3: Liver. *Ultrasound Med Biol*. 2015;41(5):1161-1179.
21. Zakrzewski AM, Huang AY, Zubajlo R, Anthony BW. Real-time blood pressure estimation from force-measured ultrasound. *IEEE Trans Biomed Eng*. 2018;65(11):2405-2416.
22. Gilbertson MW, Anthony BW. An ergonomic, instrumented ultrasound probe for 6-axis force/torque measurement. In: *Proceedings of the Annual International Conference of the IEEE Engineering in Medicine and Biology Society, EMBS*; 2013:140-143.
23. Huang AY, Anthony BW. An instrumented ultrasound probe for shear wave elastography with uneven force distribution. In: *Institute of Electrical and Electronics Engineers (IEEE)*; 2019:6208-6211.
24. Hambly NM, Gonen M, Gerst SR, et al. Implementation of evidence-based guidelines for thyroid nodule biopsy: A model for establishment of practice standards. *Am J Roentgenol*.

2011;196(3):655-660.

25. Tian W, Hao S, Gao B, et al. Comparison of diagnostic accuracy of real-time elastography and shear wave elastography in differentiation malignant from benign thyroid nodules. *Medicine (Baltimore)*. 2015;94(52):e2312.

26. Grani G, Lamartina L, Cantisani V, Maranghi M, Lucia P, Durante C. Interobserver agreement of various thyroid imaging reporting and data systems. *Endocr Connect*. 2017:EC-17-0336.

27. Monpeyssen H, Tramalloni J, Poirée S, Hélénon O, Correas J-M. Elastography of the thyroid. *Diagn Interv Imaging*. 2013;94(5):535-544.

28. Sporea I, Sirli R, Bota S, Vlad M, Popescu A, Zosin I. ARFI elastography for the evaluation of diffuse thyroid gland pathology: Preliminary results. *World J Radiol*. 2012;4(4):174-178.

29. Sedlackova Z, Herman J, Furst T, Salzman R, Vachutka J, Herman M. Shear wave elastography in diffuse thyroid disease. *Biomed Pap*. 2020;164.

30. Liu J, Zhang Y, Ji Y, Wan Q, Dun G. The value of shear wave elastography in diffuse thyroid disease. *Clin Imaging*. 2018;49:187-192.

31. Lam ACL, Pang SWA, Ahuja AT, Bhatia KSS. The influence of precompression on elasticity of thyroid nodules estimated by ultrasound shear wave elastography. *Eur Radiol*. 2016;26(8):2845-2852.

32. Cosgrove D, Barr R, Bojunga J, et al. WFUMB guidelines and recommendations on the

clinical use of ultrasound elastography: Part 4. Thyroid. *Ultrasound Med Biol*. 2017;43(1):4-26.

33. Elseedawy M, Whelehan P, Vinnicombe S, Thomson K, Evans A. Factors influencing the stiffness of fibroadenomas at shear wave elastography. *Clin Radiol*. 2016;71(1):92-95.
34. DeWall RJ, Varghese T, Kliewer MA, Harter JM, Hartenbach EM. Compression-dependent viscoelastic behavior of human cervix tissue. *Ultrason Imaging*. 2010;32(4):214-228.
35. Syversveen T, Midtvedt K, Berstad AE, Brabrand K, Strøm EH, Abildgaard A. Tissue elasticity estimated by acoustic radiation force impulse quantification depends on the applied transducer force: An experimental study in kidney transplant patients. *Eur Radiol*. 2012;22(10):2130-2137.
36. Barr RG, Zhang Z. Effects of precompression on elasticity imaging of the breast. *J Ultrasound Med*. 2012;31(6):895-902.
37. Dhyani M, Sc R, Mw G, et al. A pilot study to precisely quantify forces applied by sonographers while scanning: A step toward reducing ergonomic injury. *Work*. 2017;58(2):241-247.

Table 1: Demographics of the study population

Descriptor	Overall N=19
Age (years)	36.3 ± 8.4
Female (mean, range)	37.2, 27 – 56
Male (mean, range)	33.6, 28 – 44
Gender (%, n)	
Female	74, 14
Male	26, 5
BMI (%, n)	
Normal	74, 14
Overweight	5, 1
Obese	21, 4

Table 2: Descriptive Young's modulus values by preload force (N)

Preload Force, N	Young's Modulus [Mean, SD] (kPa)	Percentiles [25, 50, 75]
2	16.6, 5.1	13.6, 16.6, 21.4
4	19.4, 7.2	15.7, 18.7, 23.3
6	22.5, 7.5	18.0, 22.7, 27.1
8	25.5, 9.5	18.9, 25.5, 30.4
10	30.1, 12.0	20.8, 29.8, 36.9

SD: standard deviation

Table 3: Regression coefficients and linear combinations that summarize the mean Young's modulus values (kPa) for a preload force (2 - 10 N)

Descriptor	Estimate	95% CI	P-value
Regression coefficients			
Intercept	14.65	[11.5 - 17.79]	< 0.001
Force	0.92	[0.12 - 1.71]	0.027
Force^2	0.06	[0.01 - 0.11]	0.013
Estimated force mean values (N)	**Modulus**		
2	16.7	[14.1 - 19.3]	
4	19.3	[16.5 - 22.1]	
6	22.3	[19 - 25.7]	
8	25.9	[21.8 - 30]	
10	29.9	[24.9 - 34.9]	
Sequential force mean differences	**Modulus**		
4-2	2.6	[1.3 - 3.8]	
6-4	3.1	[1.91 - 4.2]	
8-6	3.5	[2.4 - 4.7]	
10-8	4	[2.8 - 5.3]	

Confidence Interval (CI)

Figure Captions

Figure 1: Force Measurement Device. This device is composed of a mechanics and electronics enclosure and a tablet with a graphical user interface, which connects to an ultrasound machine. Pictured is the GE Logiq E9 system but for this data collection the Aixplorer (Supersonic Imagine, Paris, France) was used with a SL15-4 MHz linear ultrasound transducer.

Figure 2: Shear wave elastography images of thyroid of the transverse plane. 5 different images at 5 different pressure levels (2 N - 10 N) are presented. Note the increase in estimated tissue Young's modulus (in kPA) as transducer pressure increases. The subject is female and 34 years old.

Figure 3: Summary of the relationship between preload force and stiffness (Young's modulus) values by patient. The estimated relationship using a linear mixed-effects model (black line) along with the 95% pointwise confidence band (red region).

Please wait...

If this message is not eventually replaced by the proper contents of the document, your PDF viewer may not be able to display this type of document.

You can upgrade to the latest version of Adobe Reader for Windows®, Mac, or Linux® by visiting http://www.adobe.com/go/reader_download.

For more assistance with Adobe Reader visit http://www.adobe.com/go/acrreader.

Please wait...

If this message is not eventually replaced by the proper contents of the document, your PDF viewer may not be able to display this type of document.

You can upgrade to the latest version of Adobe Reader for Windows®, Mac, or Linux® by visiting http://www.adobe.com/go/reader_download.

For more assistance with Adobe Reader visit http://www.adobe.com/go/acrreader.

Please wait...

If this message is not eventually replaced by the proper contents of the document, your PDF viewer may not be able to display this type of document.

You can upgrade to the latest version of Adobe Reader for Windows®, Mac, or Linux® by visiting http://www.adobe.com/go/reader_download.

For more assistance with Adobe Reader visit http://www.adobe.com/go/acrreader.

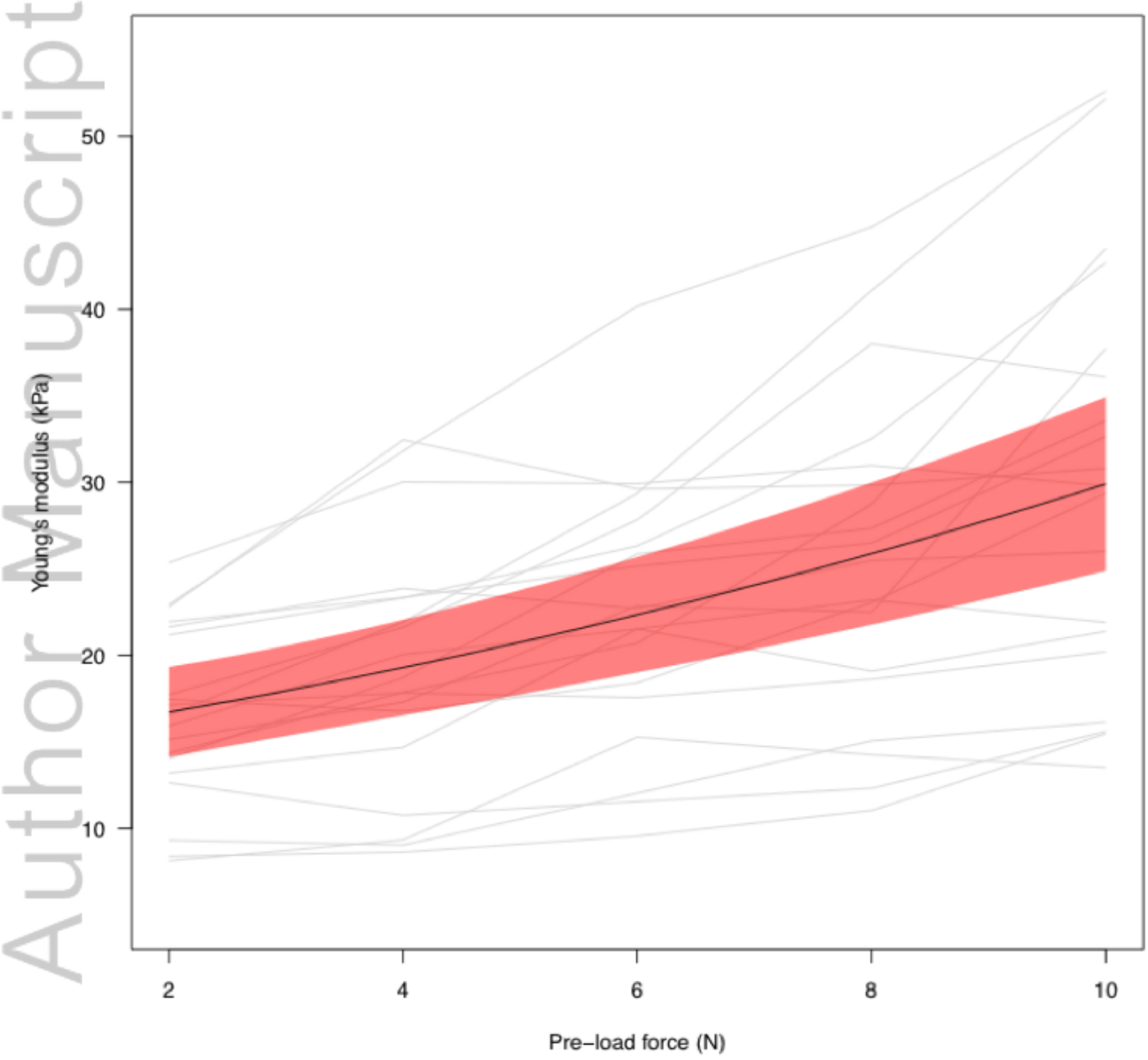

JUM_15456_Figure3_ppt_v4.png

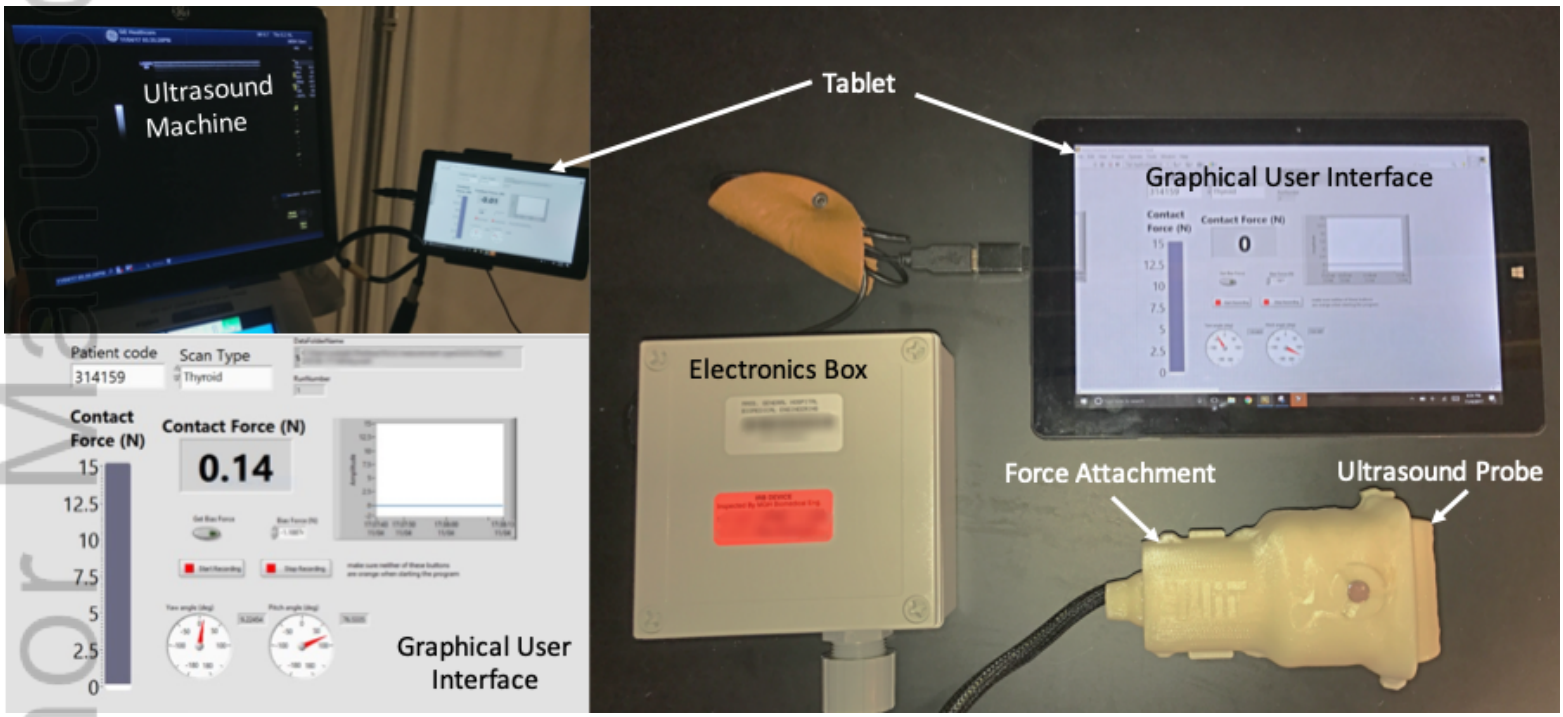

JUM_15456_Figure 1.png

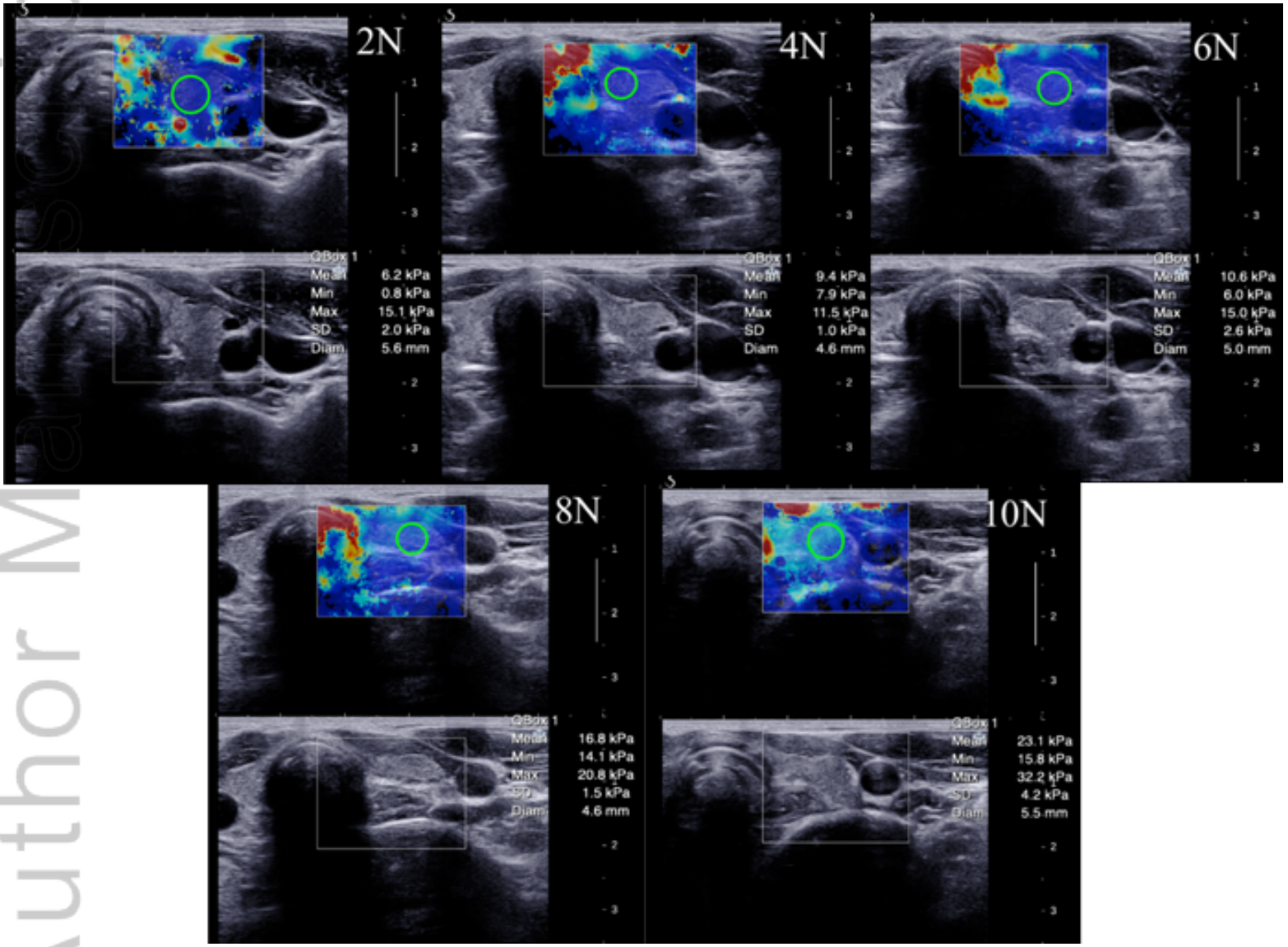

JUM_15456_Figure 2.png

Please wait...

If this message is not eventually replaced by the proper contents of the document, your PDF viewer may not be able to display this type of document.

You can upgrade to the latest version of Adobe Reader for Windows®, Mac, or Linux® by visiting http://www.adobe.com/go/reader_download.

For more assistance with Adobe Reader visit http://www.adobe.com/go/acrreader.

Please wait...

If this message is not eventually replaced by the proper contents of the document, your PDF viewer may not be able to display this type of document.

You can upgrade to the latest version of Adobe Reader for Windows®, Mac, or Linux® by visiting http://www.adobe.com/go/reader_download.

For more assistance with Adobe Reader visit http://www.adobe.com/go/acrreader.

Please wait...

If this message is not eventually replaced by the proper contents of the document, your PDF viewer may not be able to display this type of document.

You can upgrade to the latest version of Adobe Reader for Windows®, Mac, or Linux® by visiting http://www.adobe.com/go/reader_download.

For more assistance with Adobe Reader visit http://www.adobe.com/go/acrreader.

Please wait...

If this message is not eventually replaced by the proper contents of the document, your PDF viewer may not be able to display this type of document.

You can upgrade to the latest version of Adobe Reader for Windows®, Mac, or Linux® by visiting http://www.adobe.com/go/reader_download.

For more assistance with Adobe Reader visit http://www.adobe.com/go/acrreader.